One-Disulfide Intermediates of Apamin Exhibit Native-like Structure†

Xiaobing Xu and Jeffrey W. Nelson*

Department of Biochemistry, Louisiana State University, Baton Rouge, Louisiana 70803

Received November 8, 1993; Revised Manuscript Received February 23, 1994®

ABSTRACT: The conformations of three peptide models of the one-disulfide and fully reduced forms of apamin were characterized by using nuclear magnetic resonance (NMR) spectroscopy. Apa-2 contains the native disulfide bond between Cys3 and Cys15 in apamin with the other two cysteines replaced by alanines. Apa-1 contains the native disulfide bond between Cys1 and Cys11. Apa-S has all cysteines replaced with serines, mimicking fully reduced apamin. Comparing NOESY cross peaks and coupling constants for amide protons in the peptide analogs with those in native apamin indicates that a significant portion of Apa-2 possesses native-like structural elements of apamin in addition to some random coil conformations. Apa-1 contains a short helical structure from Ala9 to Arg13, corresponding to the N-terminal portion of the α-helix observed in the native structure, along with some local and probably flexible secondary structures corresponding to the reverse turn region in native apamin. A larger portion of Apa-1 exists in the form of random coil conformations compared to Apa-2. Apa-S displays mainly random coil conformations with some localized helical structures from Glu7 to Arg14 which are similar to the "nascent helices" proposed by Wright et al. [Wright, P. E., Dyson, H. J., & Lerner, R. A. (1988) *Biochemistry 27,* 7167-7175]. Formation of the first disulfide bond in apamin seems to be important in the folding process by stabilizing native-like structure, presumably by reducing the conformational freedom and initiating formation of structure. For a small peptide such as apamin, the position of the disulfide bond is important in determining the conformations of folding intermediates, as evidenced by Apa-2 exhibiting significantly more native-like conformations than Apa-1.

Apamin is a small neurotoxic peptide isolated from honey bee venom containing 18 amino acid residues and two disulfide bonds. Research on apamin has largely focused on its unusual ability to pass the blood/brain barrier and act on the central nervous system (Habermann, 1972) and its function as a specific blocker of calcium-dependent potassium channels (Banks et al., 1979). Efforts have also been made toward understanding the relationship between structure and function (Vincent et al., 1975; Granier et al., 1978; Labbe-Jullie et al., 1991; Auguste et al., 1992; Shahidi et al., 1993). The sequence of apamin is shown on the top of Figure 1. The folded conformation of apamin has been determined from NMR[1] spectroscopy by using NOE distance constraints and distance geometry calculations (Wemmer & Kallenbach, 1983; Pease & Wemmer, 1988), and consists of a type I reverse turn from residues 2 to 5 and a C-terminal α-helix from residues 9 to 17 (Pease & Wemmer, 1988).

The native structure of apamin is very stable over a very broad range of pH, temperature, and denaturants (Miroshnikov et al., 1978). The two disulfide bonds in apamin form in a very cooperative manner (Chau & Nelson, 1992): in equilibrium mixtures of reduced and oxidized apamin, one-disulfide bond intermediate states are populated to only a few percent. It is very important to characterize the properties of the folding intermediates in order to understand the folding of proteins. Therefore, we have previously characterized the disulfide bond stabilities and CD spectra of two model one-disulfide intermediates, Apa-1 and Apa-2, designed to contain one native disulfide bond by replacing one pair of cysteines with alanines (Huyghues-Despointes & Nelson, 1992). As shown in Figure 1, Apa-1 contains the disulfide bond between Cys1 and Cys11, whereas Apa-2 contains the disulfide bond between Cys3 and Cys15. The peptide Apa-S, which has all four cysteines replaced by serines and a carboxyl rather than amide C-terminus, serves as a model for fully reduced apamin (Huyghues-Despointes & Nelson, 1992). The disulfide bond in Apa-2 was found to be almost twice as stable as in Apa-1. From CD measurements, Apa-2 displays a reasonable amount of structure although significantly less than apamin. Apa-1 contains somewhat less structure, whereas Apa-S exhibits an essentially random coil CD spectrum (Huyghues-Despointes & Nelson, 1992). Therefore, CD spectra suggest that a certain amount of secondary structure is present in both of the one-disulfide intermediates of apamin.

The folding of proteins with disulfide bonds involves formation and rearrangement of disulfide bonds. Monitoring the formation of these disulfide bonds can thus be used to map out the folding process. One of the best characterized protein folding pathways is that of BPTI, a 58-residue protein containing three disulfide bonds in its native folded conformation (Creighton, 1978, 1992). The most efficient pathway of BPTI folding has been determined by measuring the kinetics and stabilities of the disulfide-bonded intermediates (Creighton & Goldenberg, 1984; Creighton, 1992). Extensive efforts have been made to characterize the conformations of one- or two-disulfide intermediates to understand their kinetic and thermodynamic behaviors. Intermediates and analogs ob-

† Financial support was provided by NIH Grant GM 39615.

* To whom correspondence should be addressed.

® Abstract published in *Advance ACS Abstracts,* April 1, 1994.

[1] Abbreviations: NMR, nuclear magnetic resonance; CD, circular dichroism; TPPI, time-proportional phase increments; TSP, trimethylsilylproponic acid; 2D, two dimensional; NOESY, two-dimensional nuclear Overhauser effect spectroscopy; DQF-COSY, two-dimensional double-quantum-filtered correlation spectroscopy; HOHAHA, two-dimensional homonuclear Hartmann–Hann spectroscopy; ROESY, rotating-frame NOESY spectroscopy; FID, free induction decay; ppm, parts per million; ppb, parts per billion; BPTI, bovine pancreatic trypsin inhibitor; TFE, trifluoroethanol; $(5\text{–}55)_{Ser}$, etc., analogs of BPTI with disulfide bonds connecting indicated cysteine pairs in parentheses, with other cysteines replaced by the amino acid subscript.

0006-2960/94/0433-5253$04.50/0

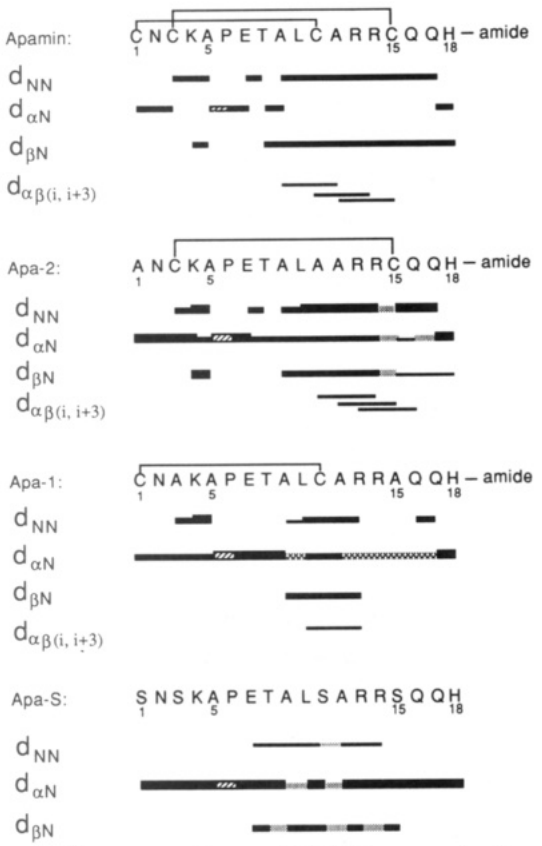

FIGURE 1: Sequences and sequential NOE cross peaks observed in NOESY spectra for apamin, Apa-2, Apa-1, and Apa-S. Lines connecting cysteines represent the disulfide bonds. Solid bars represents positively identified NOE connectivities, with the relative intensities indicated by the thickness of the bars. Slash shaded bars represent Ala5 $C^{\alpha}H$ to Pro6 $C^{\delta}H$ NOEs. Shaded bars represent possible NOEs between unresolved resonances. Cross hatches represent positively identified but partially resolved NOEs with uncertain intensities. Data for apamin are reformatted from Pease and Wemmer (1988).

tained by chemical trapping (States et al., 1987) and by synthesis of peptide models containing subdomains of native structure (Oas & Kim, 1988; Staley & Kim, 1990) have been studied by NMR. Recently, several one- and two-disulfide intermediate analogs of BPTI with cysteine residues replaced by alanines or serines have been prepared by site-directed mutagenesis and analyzed in detail by using 2D ^{1}H NMR (van Mierlo et al., 1991a,b, 1992, 1993) and X-ray crystallography (Eigenbrot et al., 1990). These studies showed that intermediate analogs $(5–55)_{Ser}$ (containing disulfide bond between Cys5 and Cys55 with other cysteines replaced by serines) and $(14–38, 5–55)_{Ala}$ assume structures most similar to native BPTI. The intermediate analog $(14–38, 30–51)_{Ser}$ contains slightly less native-like structure, whereas $(30–51)_{Ser}$ contains only partially folded conformations. The conformations of these intermediate analogs can be used to explain their kinetic roles in protein folding (van Mierlo et al., 1991a, 1992).

Compared to BPTI, apamin is a much smaller peptide. The conformations of one-disulfide intermediates of apamin are expected to be more flexible than native apamin. The solution conformations assumed by many small peptides have been characterized by using 2D ^{1}H NMR (Dyson et al., 1988a,b; Wright et al., 1988; Osterhout et al., 1989; Dyson & Wright, 1991; Kemmink et al., 1993). The conformations of small peptides typically consist of several structures rapidly interchanging. In characterizing the conformations of small linear peptides, localized partially folded structures were observed from NOE measurements and named the "nascent helix" (Dyson et al., 1988b; Wright et al., 1988; Dyson & Wright, 1991). The nascent helix is represented by an ensemble of turn-like structures over several adjacent residues of a peptide. These partially folded structures display sequential NH–NH NOE connectivities but lack medium-range NOEs characteristic of secondary structures. Although the peptides exhibiting nascent helix do not display structures in CD spectra in aqueous solution, the helix can be stabilized and observed by CD and NMR upon addition of TFE. Besides NOE measurements, other information obtained from NMR measurements such as hydrogen bonding of amide protons, spin-spin coupling constants, and chemical shifts of proton resonances can provide additional evidence about various structural elements assumed by a peptide (Dyson & Wright, 1991).

In the present study, we have characterized the structures formed in Apa-2, Apa-1, and Apa-S by using 1D and 2D NMR techniques. Their conformations were derived from patterns of NOE interactions and coupling constants. The conformations obtained for these peptides are compared with the native structure of apamin to infer the effects of disulfide bonds on the structures. The conformations obtained from NMR measurements are also compared with the results from previous CD measurements to obtain further understanding of the conformations assumed in each peptide.

MATERIALS AND METHODS

Sample Preparation. Apamin, Apa-2, Apa-1, and Apa-S were synthesized by either tBOC or Fmoc synthesis strategies and were purified and characterized as previously described (Huyghues-Despointes & Nelson, 1992). All NMR samples contained approximately 5 mM peptide, 0.1 M KCl, and 10 mM deuterated acetic acid in either 90%H_2O/10% D_2O or 99.8% D_2O and were adjusted to pH 4.0 (uncorrected pH glass electrode reading). Approximately 1 mM TSP was added to each sample to establish the chemical shift reference.

NMR spectroscopy. All NMR experiments were carried out on a Bruker AMX-500 MHz spectrometer. 2D NMR spectra were typically collected as 700 t_1 increments, with 2048 complex points collected in t_2. The sweep width was 6024 Hz in both dimensions. TPPI was used for phase-sensitive detection in t_1 in all 2D spectra (Marion & Wüthrich, 1983). Irradiation of the water peak was used for solvent suppression for most 1D and 2D experiments. DQF-COSY (Marion & Wüthrich, 1983; Rance et al., 1983) spectra were typically collected with 16 transients per t_1 increment. HOHAHA (Bax & Davis, 1985; Davis & Bax, 1985) spectra were collected with an MLEV-17 spin lock field of approximately 7 kHz, a mixing time of 70 ms, and eight transients per t_1 increment. For measuring the spin–spin couping constants for Apa-1 and Apa-2, HOHAHA spectra with 1024 t_1 increments and 4096 complex points in t_2 were collected in order to achieve high spectral resolution. Phase-sensitive NOESY (Jeener et al., 1979; Bodenhausen et al., 1984) spectra were collected at mixing times 150, 300, and 450 ms, with 32 transients per t_1 increment. NOESY spectra with a jump–return sequence (Hore, 1983) were taken with a 300-ms mixing time. ROESY (Bothner-By et al., 1984) spectra were collected with a spin lock field of approximately 2 kHz, a mixing time of 150 ms, and 32 transients per t_1 increment.

In processing the 2D data, FIDs in the t_2 dimension were apodized by using a 45° phase-shifted sine-bell function. In the t_1 dimension the data were zero-filled to 2048 complex points before applying a 90°-shifted sine-bell apodization.

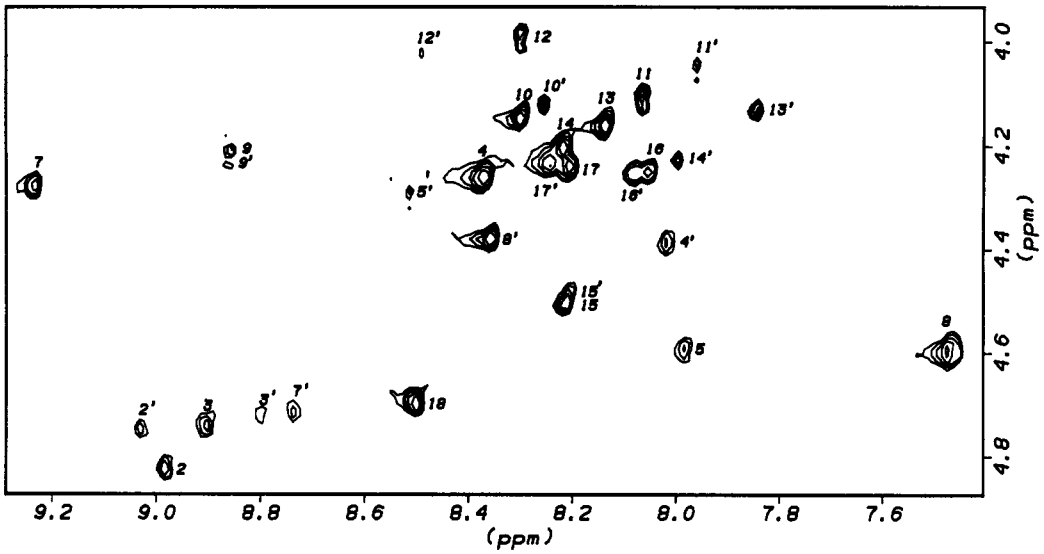

FIGURE 2: Fingerprint region of the HOHAHA spectrum of Apa-2 taken in 10%D_2O/90%H_2O at 5 °C and pH 4.0. Each peak is labeled with the residue number. Cross peaks labeled with primed numbers (′) represent signals from the *cis* isomer of the Pro6 peptide bond.

The first row of the matrix was multiplied by 0.5 before t_1 transformation to suppress t_1 ridges (Otting et al., 1986). In processing the 1D data, spectra were zero-filled and Gaussian window apodizations were used to enhance the resolution. The processed 1D spectra had a resolution of 0.37 Hz/point to facilitate the measurement of coupling constants. All data processing was done by using the FELIX program (Hare Research Inc.) running on a Silicon Graphics Personal Iris workstation. The TSP peak was used as chemical shift reference without correcting the effects of temperature or pH.

Complete sets of 2D NMR spectra were taken for Apa-1, Apa-2, and Apa-S. These include NOESY spectra collected at 5 °C using mixing times of 150, 300, and 450 ms, jump–return NOESY spectra (300-ms mixing time) and DQF-COSY spectra at 5 °C, ROESY, DQF-COSY, and NOESY (300-ms mixing time) spectra at 25 °C, and HOHAHA spectra at 5, 15, and 25 °C. For apamin, only NOESY and HOHAHA spectra were collected at 5 °C for chemical shift comparisons.

RESULTS

NMR Resonance Assignments. The complete sequential assignments of Apa-1, Apa-2, Apa-S, and apamin were obtained by using the procedures developed by Wüthrich et al. (Billeter et al., 1982; Wagner & Wüthrich, 1982; Wüthrich et al., 1982; Wüthrich, 1986). For Apa-1 and Apa-2, more resonances are observed in both fingerprint and aliphatic regions than expected. Figure 2 shows the fingerprint region of the HOHAHA spectrum for Apa-2 at 5 °C. Although Apa-2 has only 16 backbone amides, almost twice that many resonances are observed in the fingerprint region. Peptide aggregation is unlikely to be responsible for the extra resonances, since NMR spectra and NOE cross peaks measured at 1 and 5 mM peptide concentrations are very similar. The extra resonances can be attributed to the presence of both *cis* and *trans* isomers of the Pro6 peptide bond. The existence of both *cis* and *trans* isomers was confirmed by the observed NOEs between Ala5 and Pro6. A strong NOE cross peak is observed between $C^{\alpha}H$ of Ala5 and $C^{\delta}H$ of Pro6 indicative of the *trans* isomer, whereas a strong NOE cross peak is observed between $C^{\alpha}H$ of Ala5 and $C^{\alpha}H$ of Pro6 for the *cis* isomer. As seen in Figure 2, every backbone amide and C^{α} proton resonance for both isomers can be positively identified. For Apa-2, 91% of the side chain resonances in the *trans* isomer and 61% in the *cis* isomer can be assigned unambiguously. For Apa-1, due to the severe spectral congestion and small population of the *cis* isomer, most resonances in the *trans* isomer and a few backbone resonances in the *cis* isomer from residues 9 to 14 can be positively assigned on the basis of NOE connectivities. Rough estimations of the relative populations of the *cis* and *trans* isomers were obtained from the intensities of the same resonances in 1D spectra. The data indicate that the *cis* isomer comprises about 20–25% in Apa-2 and 10–15% in Apa-1. Surprisingly, for Apa-S at 5 °C, the *trans* isomer is the predominant species. A very small amount of the *cis* isomer is observed at 25 °C for Apa-S. For apamin, only the *trans* isomer is observed. The chemical shifts of all the resonances for Apa-2, Apa-1, Apa-S, and apamin are reported in the supplementary material. Since there are no complete data available for the *cis* isomers, they are not tabulated. Apamin displays large chemical shift differences from previously reported values (Wemmer & Kallenbach, 1983), which were taken at pH 2 and 25 °C, especially for amides of Asn2 and Glu7. The large chemical shift difference for these two resonances are mainly due to the pH difference (pH 2 vs pH 4) as reported previously (Bystrov et al., 1980; Dempsey, 1986).

Conformations of Model Intermediates. Figure 1 shows a comparison of NOEs observed in the NOESY spectra for apamin, Apa-2, Apa-1, and Apa-S (for the *trans* isomers). In all peptides except apamin, consecutive $C^{\alpha}H$–NH NOEs are observed throughout the peptide sequence, indicating the existence of extended or random coil conformations in these three peptides. However, each peptide also reveals many structurally informative NOEs. The NH–NH regions of NOESY spectra for Apa-2, Apa-1, and Apa-S are shown in Figure 3, panels a–c, respectively. It is apparent that consecutive NH–NH NOE connectivities are observed in all three peptides. In general, the NMR data indicate that the solution conformations of these peptides are dynamic, with both structured and random coil conformations present. The conformational transitions occur faster than the NMR time scale, since only one set of chemical shifts are observed. The details of the structured conformations for each peptide are discussed below.

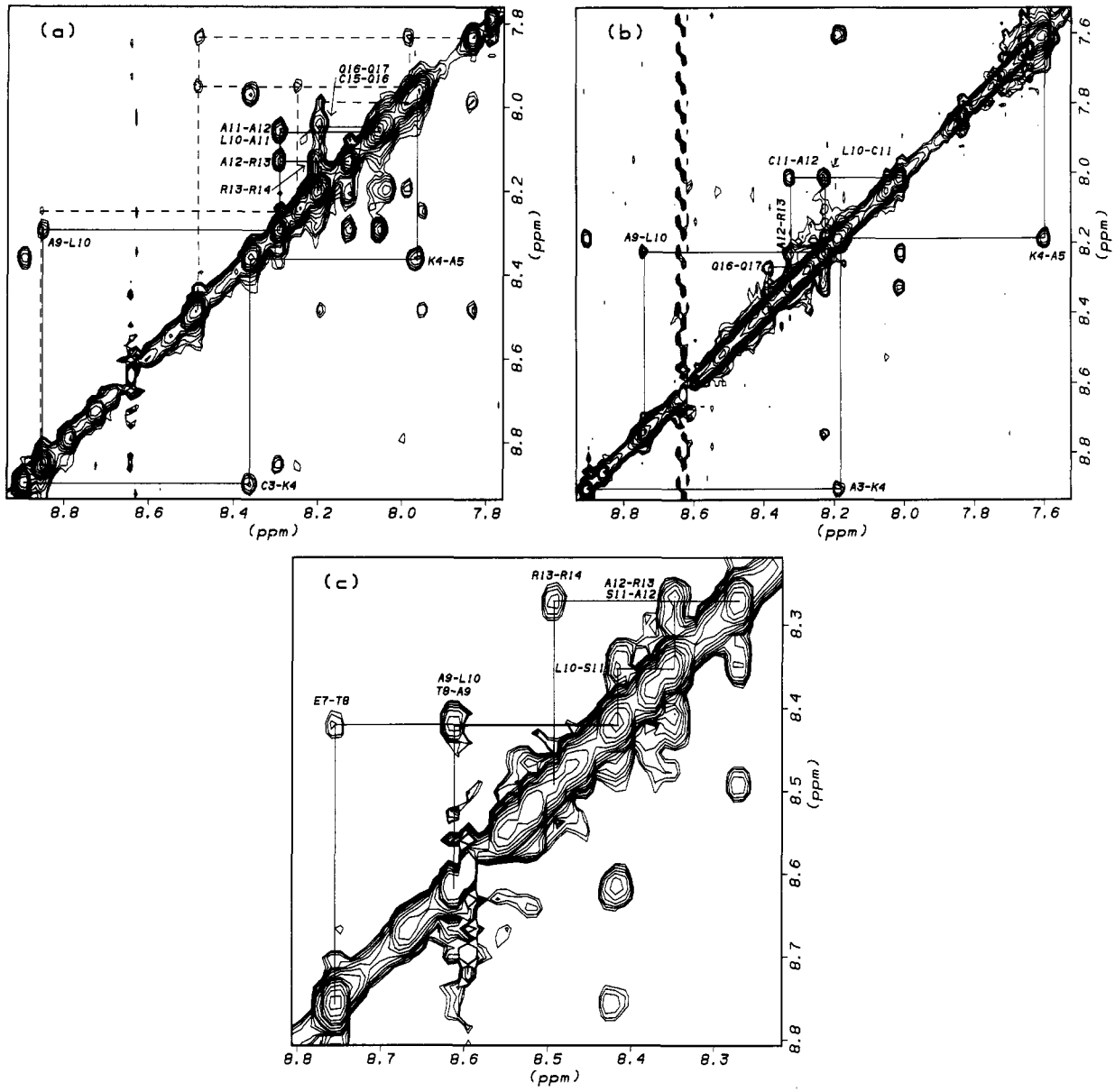

FIGURE 3: Amide–amide region of NOESY spectra taken in 10%D_2O/90%H_2O at 5 °C and pH 4.0, using a mixing time of 300 ms, for (a) Apa-2, (b) Apa-1, and (c) Apa-S. Solid lines indicate NH–NH connectivities for the *trans* isomers. Only NOE cross peaks for the *trans* isomers are labeled. Dashed lines indicate NH–NH connectivities for the *cis* isomer of Apa-2 in panel a.

For Apa-2, consecutive NH–NH NOEs are observed from Ala9 to Gln17 (Figure 3a), and consecutive $C^{\beta}H$–NH NOEs are also observed from Ala9 to His18. This suggests a substantial amount of α-helical conformation for Apa-2 from Ala9 to Gln17. In the aliphatic region of the NOESY spectrum shown in Figure 4, several medium-range NOEs from $C^{\alpha}H(i)$ to $C^{\beta}H(i+3)$ are detected. The observation of NOE interactions between $C^{\alpha}H(11)$ and $C^{\beta}H(14)$, $C^{\alpha}H(12)$ and $C^{\beta}H(15)$, and $C^{\alpha}H(13)$ and $C^{\beta}H(16)$ confirms an α-helical structure in this region. From Asn2 to Ala5, the NOE pattern observed is similar to that in apamin and represents a type I reverse turn. From a comparison of the NOEs observed for apamin and Apa-2, it appears that the NOE interactions in Apa-2 are very similar to those of apamin (except for $C^{\alpha}H$–NH NOEs arising from unstructured populations), suggesting that the helical and turn structural elements are very similar for these two peptides.

For Apa-1, fewer NH–NH NOEs are observed compared to Apa-2 (see Figures 1 and 3a,b). From Ala3 to Ala5, NH–NH NOEs are observed with the intensity between residues 4 and 5 stronger than that between residues 3 and 4, suggesting a possible type I reverse turn. However, no other NOEs are observed to support the turn structure, indicating that this part of the peptide may be more flexible or less stable than the turn in Apa-2. From Ala9 to Arg13, consecutive NH–NH and $C^{\beta}H$–NH NOEs are observed, suggesting a short helical conformation from Ala9 to Arg13. One NOE from the $C^{\alpha}H$ of Leu10 to the $C^{\beta}H$ of Arg13 is also observed, suggesting the existence of an α-helical structure in that region. This short helical structure corresponds to the N-terminal portion of the α-helix found in native apamin (Pease & Wemmer, 1988).

For Apa-S, in addition to the strong $C^{\alpha}H$–NH NOEs observed through the entire peptide, consecutive NH–NH and $C^{\beta}H$–NH NOEs are also detected from Glu7 to Arg14 (Figure 3c). The relative intensities for NH–NH NOEs are much weaker than $C^{\alpha}H$–NH NOEs. These results indicate that a small portion of the peptide forms local helical structures from Glu7 to Arg14. No medium-range NOE interactions from $C^{\alpha}H(i)$ to $C^{\beta}H(i+3)$ are observed, suggesting a very flexible helical structure. This structure exhibits the properties of the "nascent helix" proposed by Wright et al. (Dyson et al.,

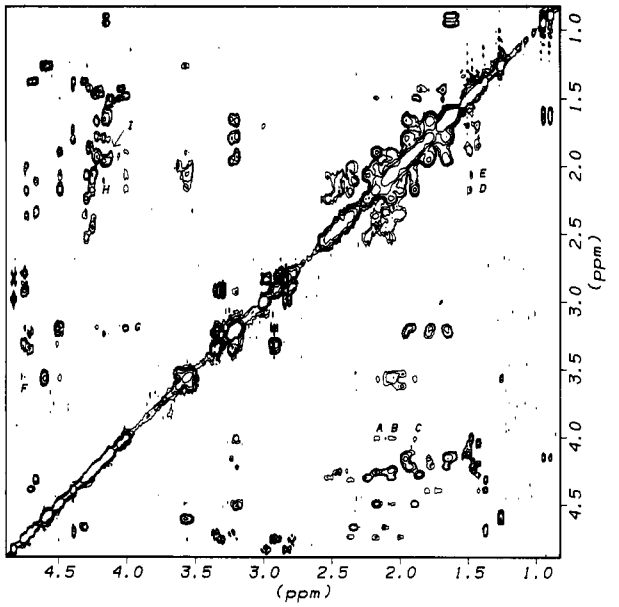

FIGURE 4: Aliphatic region of the NOESY spectrum of Apa-2 taken in 100% D_2O at 5 °C and pH 4.0, using a mixing time of 300 ms. Structurally informative NOEs are labeled on the figure with letters A–I: (A) $C^{\alpha}H(12)$–$C^{\beta}H(6)$; (B) $C^{\alpha}H(12)$–$C^{\gamma}H'(6)$; (C) $C^{\alpha}H(12)$–$C^{\beta}H'(6)$; (D) $C^{\beta}H(6)$–$C^{\beta}H(11)$; (E) $C^{\beta}H(12)$–$C^{\gamma}HH'(6)$; (F) $C^{\alpha}H(3)$–$C^{\delta}HH'(6)$; (G) $C^{\alpha}H(12)$–$C^{\beta}HH'(15)$; (H) $C^{\alpha}H(13)$–$C^{\beta}H'$-(16); (I) $C^{\alpha}H(11)$–$C^{\beta}H(14)$.

1988b; Wright et al., 1988; Dyson & Wright, 1991). This result is particularly interesting considering that there is no disulfide bond in this peptide. Apparently there is a small tendency for forming local helical structures even in fully reduced apamin.

Conformations of One-Disulfide Intermediates from Coupling Constants. The coupling constant $^3J_{HN\alpha}$ for each amide proton can be used to deduce dihedral angles (Pardi et al., 1984; Wüthrich, 1986). These coupling constants in the peptide analogs were measured from 1D spectra, or 2D HOHAHA spectra in cases where peaks cannot be resolved in 1D spectra. The results are listed in Table 1. Coupling constants for apamin (Bystrov et al., 1980) are also shown for comparison. For Apa-2, the coupling constants from Asn2 to Ala5 are 8.1, 4.9, 6.9, and 8.8 Hz, a typical pattern for a type I reverse turn. From Ala9 to Gln17, the coupling constants are consistently small, consistent with an α-helical structure in this region. The overall coupling constant patterns for Apa-2 and apamin are remarkably similar, suggesting similar conformations between them. For Apa-1, the coupling constants from Ala9 to Arg13 are all less than 4.5 Hz, consistent with an α-helical structure in this region. For other residues, no pattern corresponding to local secondary structure elements can be established. The coupling constants observed for Apa-S are generally in the neighborhood of 6 Hz, which is higher than that for α-helix and lower than that for extended β-sheet structures. These data indicate that the major portion of Apa-S is in random coil conformations. Although coupling constants are not strong evidence for structure (Dyson & Wright, 1991), the conformations obtained from coupling constants are consistent with those derived from NOE measurements for each peptide.

Hydrogen Bond Formation. The possibilities for intrapeptide hydrogen bond formation involving amide protons of Apa-2, Apa-1, and Apa-S were evaluated from the temperature dependence of amide proton chemical shifts. The data are listed in Table 2. The formation of an intrapeptide hydrogen bond due to the formation of secondary structure will typically result in a small value for the temperature dependence of the chemical shift of the hydrogen-bonded amide proton (Dyson et al., 1988a). As shown in Table 2, several amide protons of Apa-2 have very small temperature coefficients (≤3.0 ppb/K): Lys4, Ala5, Thr8, Cys15, Gln16 and Gln17. This suggests that these amide protons are possibly involved in hydrogen bonding. A few amide protons of Apa-1 have very small temperature coefficients (≤2.5 ppb/K): Lys4, Ala5, Thr8, and Cys11. Ala5 is in a reverse turn, and its amide is possibly hydrogen bonded to the backbone carbonyl oxygen of Asn2. The Lys4 amide is possibly involved with a hydrogen bond with the oxygen atom from the side chain of Asn2. Both of these hydrogen bonds were observed in native apamin (Pease & Wemmer, 1988). The observation of hydrogen bonds involving Cys15, Gln16, and Gln17 in Apa-2 is consistent

Table 1: Coupling Constants for Apa-2, Apa-1, Apa-S, and Apamin[a]

residues	Apa-2 (Hz)	Apa-1 (Hz)	Apa-S (Hz)	apamin (Hz)[b]
C1				
N2	8.1	4.4	7.2	9.5
C3	4.9	(3.7)[c]	5.3[d]	5.2
K4	6.9	8.3	4.6	7.6
A5	8.8	8.2	5.1	6.8
P6				
E7	7.0	4.3	6.3	6.9
T8	8.8	9.0	6.6	8.5
A9	2.8	3.0	4.1	2.7
L10	3.2	2.8	6.6	5.5
C11	(4.2)[c]	4.5	5.8[d]	5.9
A12	3.1	4.4	5.8	3.0
R13	3.2	4.4	6.2	4.2
R14	4.0	5.9	6.8	3.5
C15	2.8	(4.1)[c]	5.3[d]	5.4
Q16	3.6	5.0	4.2	6.8
Q17	5.3	5.9	7.2	7.1
H18	6.5	7.3	8.0	7.9

[a] Most coupling constants were obtained from 1D spectra for Apa-2, Apa-1, and Apa-S. Coupling constants for amide protons which have severe spectral overlap were obtained from HOHAHA spectra. [b] Apamin data are adopted from measurements by Bystrov et al. (1980) at 14 °C and pH 2.9. [c] Values in parentheses correspond to alanine substitutions for cysteines in Apa-1 and Apa-2. [d] Underlined values correspond to serine substitutions for cysteines in Apa-S.

Table 2: Temperature Dependence of Amide Proton Chemical Shifts for Apa-2, Apa-1, and Apa-S[a]

residues	Apa-2 (ppb/K)	Apa-1 (ppb/K)	Apa-S (ppb/K)
C1			
N2	6.5	8.0	8.0
C3	10.5	(11.5)[b]	9.5[c]
K4	3.0	2.5	9.0
A5	2.5	1.5	11.0
P6			
E7	13.0	15.0	9.0
T8	2.5	1.5	12.0
A9	12.5	10.5	12.0
L10	10.0	7.0	11.0
C11	(5.0)[b]	0.5	9.0[c]
A12	8.0	7.5	9.0
R13	4.5	5.0	7.0
R14	4.5	4.0	9.5
C15	1.0	(3.5)[b]	9.0[c]
Q16	−1.0	3.5	7.5
Q17	1.0	4.5	7.0
H18	3.5	6.5	10.5

[a] Obtained by measuring chemical shifts of amide protons at 5, 15, and 25 °C for Apa-1, Apa-2, and Apa-S from HOHAHA spectra. [b] Values in parentheses correspond to alanine substitutions for cysteines in Apa-1 and Apa-2. [c] Underlined values correspond to serine substitutions for cysteines in Apa-S.

with helical structure from residue 9 to 17. However, in Apa-1 only the amide resonance of Cys11 has a very small temperature dependence. This is consistent with a relatively small portion of the peptide assuming a well defined secondary structure or with helical structure that is not as stable as in Apa-2. In contrast, the chemical shift of every amide in Apa-S has a relatively large temperature dependence (≥7.0 ppb/K), suggesting the absence of hydrogen bonding due to secondary structure formation.

DISCUSSION

Conformations of Apa-2. The experimental results show that both NOE interactions and coupling constants for Apa-2 are very similar to those in apamin. Does some fraction of Apa-2 molecules possess a three-dimensional structure similar to native apamin? Or alternatively, do Apa-2 molecules possess only portions of secondary structure segments found in native apamin? Since information obtained from NMR cannot distinguish between the overall structured conformations and local secondary structures, it is important to analyze the conformations of Apa-2 in detail. We believe that a fraction of Apa-2 molecules adopt a structured conformation similar to the structure of native apamin for the following reasons.

All of the long-range NOEs which are essential in determining the three-dimensional structure of apamin are observed in Apa-2, particularly the important NOEs between Ala12 and Pro6. In fact, these are the only long-range NOEs observed in native apamin (Pease & Wemmer, 1988). As shown in Figure 4, NOEs between Ala12 C^{α} proton and Pro6 ring protons are easily identified in Apa-2. NOEs between Ala12 C^{β} methyl protons and Pro6 C^{γ} protons are also detected. These results indicate that the tertiary interactions observed in apamin also exist in Apa-2. If only local segments of secondary structures form, these long-range NOEs are not likely to be observed.

The coupling constant data also support the idea that a portion of Apa-2 molecules assume a native-like structure. The coupling constants $^3J_{NH\alpha}$ are measures of the dihedral angles averaged over all possible conformations. If Apa-2 forms only local secondary structure elements, the coupling constants should be very different from those of apamin, especially for the region connecting two secondary structure elements. The coupling constants observed for Apa-2 are in the expected range for both reverse turn and α-helical segments. For loop residues Glu7 and Thr8, the coupling constants for both Apa-2 and apamin are remarkably similar (see Table 1), suggesting that the relative positions of the reverse turn and the α-helical regions are very similar in these two peptides.

Comparison of CD and NMR. The conformations obtained for Apa-2, Apa-1, and Apa-S from NMR can be compared to those from CD measurements (Huyghues-Despointes & Nelson, 1992). The CD spectrum of Apa-2 displays significantly less structure than that of native apamin. The CD spectrum of Apa-1 displays less structure than that of Apa-2, whereas the CD spectrum of Apa-S resembles that of random coil conformations. The mean residue ellipticity at 222 nm can be used to roughly estimate the α-helix percentage in each peptide by using the simple linear correlation found by Zhong and Johnson (1992). From CD spectra, the mean residue ellipticity at 222 nm is approximately −19 200, −8 500, and −3 400 deg·cm^2·dmol^{-1} for apamin, Apa-2, and Apa-1, respectively. Assuming that a value of −33 000 deg·cm^2·dmol^{-1} represents 100% helix (Zhong & Johnson, 1992), these values correspond to α-helix contents of roughly 60%, 25%, and 10% for apamin, Apa-2, and Apa-1, respectively. CD data indicate that the α-helix content in Apa-2 is significantly less than in apamin. However, NMR data appear to indicate that Apa-2 possesses an overall structure very similar to apamin. This discrepancy indicates the presence of multiple conformations for this peptide. NMR measurements are site-specific and sensitive in detecting local secondary structures in the presence of random coil conformations, whereas CD spectra provide an average over all the conformations.

It is possible to estimate the relative contributions of structured and unstructured populations by combining both CD and NMR data, assuming CD measurements accurately represent the α-helical contents. In Apa-2, CD data show that, on average, about 4.5 out of 18 residues are in helical structure (corresponding to 25% helix content), while NMR data indicate that 9 out of 18 residues are in an α-helix in the structured conformations. Taken together, these data suggest that about 50% of the peptide is in a structured conformation. In the same way we can estimate that about 45% of Apa-1 is in a structured conformation, assuming that the helix in Apa-1 runs from Ala9 to Arg13. However, since CD is not sensitive in detecting unstable local structure, as evidenced by Apa-S, the above method may underestimate the structured conformation. This method is also subject to the accuracy of estimating the α-helix contents from CD measurements and the assumption of a single structured conformation. The relative portion of random coil conformations can also be roughly estimated by comparing C^{α}H–NH and NH–NH NOE intensities for the same resonance in the α-helical region. For 100% α-helical structure, strong NH–NH NOEs should be observed, whereas the C^{α}H–NH NOEs should be weak or unobservable. For an 100% random coil conformation, only strong C^{α}H–NH NOEs should be observed. The relative intensities of these two NOE cross peaks are probes of relative populations of different conformations. However, since NOE intensity is strongly dependent on interatomic distance, which will not be fixed in flexible conformations, it is not clear that we can determine the relative populations of conformations quantitatively. Nevertheless, we can depict a qualitative conformational picture for each peptide by combining the CD and NMR results.

In Apa-2, three types of conformations possibly exist in the equilibrium mixture. A portion of Apa-2 probably forms native-like structure, as discussed above. Another portion of Apa-2 molecules adopt extended or random coil conformations. It is also possible that a portion of Apa-2 molecules contain only localized segments of secondary structure, but these cannot be distinguished due to the background from highly structured and random coil conformations. In Apa-2, strong NH–NH NOEs and medium to weak C^{α}H–NH NOEs are observed in the α-helical region of the peptide, indicating that a significant portion of the peptide is in structured conformations.

Apa-1 exhibits a larger portion of random coil conformations than Apa-2, since the NH–NH NOE cross peaks are weaker than the corresponding C^{α}H–NH NOEs in the α-helical region. Thus, a small portion of the peptide is in structured conformations with helical structure from Ala9 to Arg13, corresponding to the N-terminal segment of the α-helix in native apamin. A reverse turn forms from residues 2 to 5, but is probably more flexible than the native turn, since only NH–NH NOEs are observed. From Gln16 to Gln17, a medium intensity NH–NH NOE is observed, suggesting the possible existence of a local nascent helical structure involving these

residues of the peptide. Overall, all of the data indicate that the tendency for forming native-like secondary structural elements for Apa-1 is much smaller than that for Apa-2.

In the case of Apa-S, the majority of the peptide is in random coil conformations as shown by the CD spectrum and strong $C^{\alpha}H$–NH NOEs throughout the peptide. A small portion of the peptide contains nascent helical conformations which give rise to the weak NH–NH NOEs from Glu7 to Arg13. The CD spectrum of Apa-S displays a characteristic spectrum of random coil, and no medium-range NOEs characteristic of α-helical structure are observed, substantiating the existence of only the nascent helices and the absence of well-defined folded structure. Interestingly, a tendency for helix formation exists in all three peptides to various extents for residues 9–13.

Conformations of the cis Isomers. The *cis* isomer of the Pro6 peptide bond of Apa-2 also exhibits many structurally informative NOEs. In Figure 3a, the dashed lines connect consecutive NH–NH NOEs from Ala9 to Gln17. Consecutive $C^{\beta}H$–NH NOEs are also observed in the corresponding region, suggesting a similar α-helical structure in the *cis* isomer as in the *trans* isomer. The observation of a medium-range NOE from $C^{\alpha}H$ of Cys11 to $C^{\beta}H$ of Arg14 adds additional support. However, the reverse turn was not observed in the *cis* isomer of Apa-2, since no NH–NH NOEs were observed from residues 2 to 5. The temperature dependence of the chemical shift for the NH of Ala5 shows a value of 9.0 ppb/K in the *cis* isomer versus 2.5 ppb/k in the *trans* isomer, suggesting the possible absence of a hydrogen bond involving this amide proton in the *cis* isomer. The temperature coefficients of amide resonances for Arg13–Gln17 in the *cis* isomer are less than 2.5 ppb/K (data not shown), suggesting possible hydrogen bonding involving these amide protons. These data are consistent with α-helical structure in the region from Ala9 to Gln17 in the *cis* isomer. The population of *cis* isomer is significantly increased at lower pH. At pH 2.3, about 50% of Apa-2 is in the *cis* isomer at 5 °C from the NMR measurements (data not shown). Interestingly, the *cis* isomer seems to be stabilized by the structures formed in Apa-2 at low pH. For the *cis* isomer of Apa-1, only a couple of NH–NH NOEs were observed in the helical region, suggesting only a slight tendency for helix formation in the *cis* isomer. Most of the amide protons in the *cis* isomer of Apa-1 have small chemical shifts dispersion and cannot be assigned. Therefore, the *cis* isomer of Apa-1 seems to be significantly less structured than the *trans* isomer.

Importance of Disulfide Bonds in the Folding of Apamin. The conformations of Apa-2, Apa-1, and Apa-S can provide information to evaluate the importance of forming the first disulfide bond in the folding of apamin. A significant portion of Apa-2 probably assumes a conformation similar to the native structure. A small portion of Apa-1 contains a short helical segment from Ala9 to Arg13 with a flexible reverse turn from residues 2 to 5. Apa-S is predominantly in random coil conformations with some nascent helices from Glu7 to Arg13. It is apparent that the formation of the first disulfide bond is very important in promoting structures in the folding intermediates. The disulfide bond between Cys3 and Cys15 results in more native-like structure than that between Cys1 and Cys11. The position of the disulfide bond seems to play an important role in initiating and stabilizing the native structure.

Correlations between Chemical Shift and Secondary Structures. Chemical shifts of amide and C^{α} protons are sensitive indicators of local structure. Structure formation in a peptide usually results in the chemical shifts deviating from

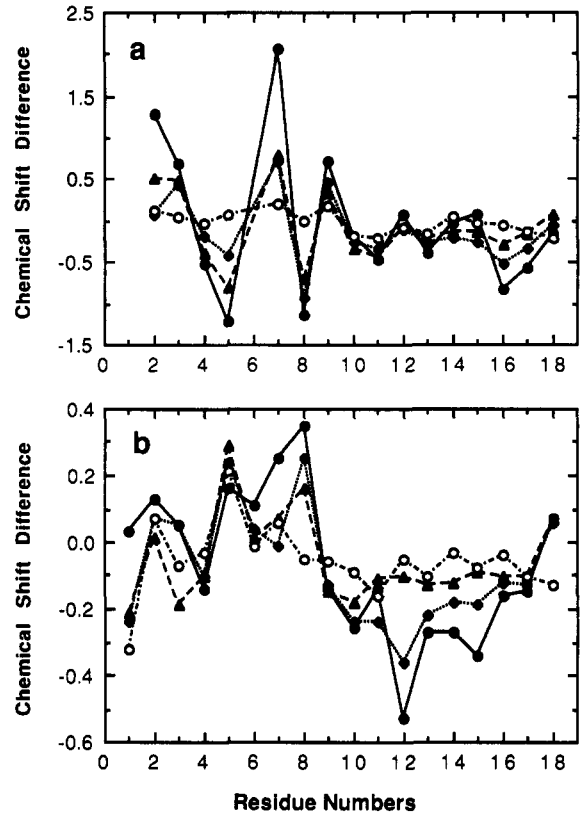

FIGURE 5: Chemical shift differences from the random coil values for (a) amide proton resonances and (b) C^{α} proton resonances of Apa-2 (◆), Apa-1 (▲), Apa-S (○), and apamin (●). The chemical shift differences were calculated using the random coil numbers from Wüthrich (1986). For amide protons, the random coil values were corrected by using a temperature dependence of 5 ppb/K to obtain the values at 5 °C. In cases of alanine and serine replacements, random coil values of alanine and serine were used, respectively.

their random coil values. The chemical shift differences for amide and C^{α} proton resonances from their random coil values (Bundi & Wüthrich, 1979; Wüthrich, 1986) for apamin, Apa-2, Apa-1, and Apa-S are plotted in Figure 5. In Figure 5a, the amide proton chemical shift differences for Apa-S are close to zero, consistent with the dominance of random coil conformations. The amide proton chemical shifts for apamin differ from the random coil values to the largest extent, indicating the largest extent of structure. It is interesting to note that in the reverse turn region in apamin, from residues 2 to 5, the amide resonances for the first two residues shift downfield (δ values increase), while the next two resonances shift upfield. However, there seems to be no obvious correlation in the α-helical region. In contrast, there is a distinctive correlation between C^{α} proton chemical shift changes and secondary structure in the α-helical region (see Figure 5b). The resonances of the C^{α} protons are shifted upfield from their random coil values in the region from residues 9 to 17 (except for C11), the α-helical region in apamin. In the sequence from Apa-S → Apa-1 → Apa-2 → apamin, the chemical shifts for the C^{α} protons move progressively upfield. The amount of upfield shift for the C^{α} proton resonances seems to increase with the amount of α-helical structure in these peptides. This observation is consistent with the conclusions obtained from statistical studies of the relationship between C^{α} proton chemical shift and secondary structures (Wishart et al., 1991).

Effects of Alanine and Serine Substitutions. In our study, model intermediates were used to infer the conformations of authentic intermediates. In the one-disulfide intermediate

analogs Apa-1 and Apa-2, a pair of cysteines were replaced by alanines. In Apa-S, all cysteines were replaced by serines. The effects of these substitutions on the conformations relative to the authentic entities need to be considered. Alanine is smaller than cysteine and has higher propensity for α-helix formation (O'Neil & DeGrado, 1990). Such replacements could potentially increase the helical structure compared to the true folding intermediate. Since serine is considered to have less propensity for α-helix formation than cysteine (Chou & Fasman, 1974; Levitt, 1978; O'Neil & DeGrado, 1990), Apa-S might contain less helical structure than fully reduced apamin. The small amount of helical structure we observe in Apa-S is therefore probably not a result of the substitution by serines. Although we cannot estimate to what extent the conformations of model peptides mimic those of true intermediates, it is reasonable to conclude that the conformations of model peptides represent the general conformational features in the true intermediates.

It is interesting to compare our results with similar studies on one- and two-disulfide intermediates of BPTI. BPTI is a somewhat larger protein (58 residues) and contains three disulfide bonds. The conformations of several folding intermediate analogs have been studied by ^{1}H NMR: $(5–55)_{Ser}$ (van Mierlo et al., 1991a), $(14–38, 30–51)_{Ser}$ (van Mierlo et al., 1991b), and $(30–51)_{Ser}$ (van Mierlo et al., 1992, 1993). It was found that the disulfide intermediates $(5–55)_{Ser}$ and $(14–38, 30–51)_{Ser}$ are both very native like, with $(5–55)_{Ser}$ being more native-like. The intermediate analog $(30–51)_{Ser}$ contains only partially folded structures which are similar to the native structure. The most native-like structure was observed in $(5–55)_{Ser}$, which was attributed to the disulfide bond reducing the conformational entropy of the unfolded state to the greatest extent since this disulfide bond connects the two cysteines furthest apart in the sequence (van Mierlo et al., 1991a). The structures of the one- and two-disulfide intermediates of BPTI are stabilized by hydrophobic interactions, since they are greatly destabilized by urea (Creighton, 1977). In our study, the position of the disulfide bond was also found to be important in promoting the native-like structures in one-disulfide intermediates of apamin. In contrast to BPTI, the structure and stability of the one-disulfide intermediates of apamin are not extensively destabilized by urea (Huyghues–Despointes & Nelson, 1992; Chau & Nelson, 1992).

The conformations of Apa-2, Apa-1, and Apa-S provide structural information toward an understanding of the folding of apamin. In fully reduced apamin, small amounts of local helical structures or nascent helices exist, which possibly promote structures conducive for forming the first disulfide bond. Formation of the first disulfide bond is accompanied by the formation of local secondary structure, perhaps by reducing the conformational freedom and thus initiating the structure formation. The disulfide bond between Cys3 and Cys15, as in Apa-2, is most stable and effectively stabilizes the structure, resulting in native-like conformations. These native-like structures greatly promote the stability of the second disulfide bond, explaining the extensive cooperativity observed in apamin folding (Chau & Nelson, 1992).

What stabilizes the structures observed in Apa-2 and apamin? It is surprising that Apa-2 exhibits so much structure. Hydrophobic stabilization is probably not significant, since urea does not greatly destabilize the structure or disulfide bond of either Apa-2 (Huyghues–Despointes & Nelson, 1992) or apamin (Chau & Nelson, 1992). Thus, apamin represents a new paradigm for the stability of protein structures in which interactions other than the hydrophobic effect are most important in stabilizing the structure.

ACKNOWLEDGMENT

We thank Laura G. Cooper for synthesizing some of the peptides used in this work. The Bruker AMX-500 NMR was purchased with funds from Louisiana Educational Quality Support Fund Grant (1987–88)-ENH-BS-3 and NIH Shared Instrumentation Grant RR 04904.

SUPPLEMENTARY MATERIAL AVAILABLE

Four tables listing the chemical shifts of all the resonances for Apa-2, Apa-1, Apa-S, and apamin at 5 °C and pH 4.0 (4 pages). Ordering information is given on any current masthead page.

REFERENCES

Auguste, P., Hugues, M., Mourre, C., Moinier, D., Tartar, A., & Lazdunski, M. (1992) *Biochemistry 31*, 648–654.
Banks, B. E. C., Brown, C., Vurgess, G. M., Burnstock, G., Claret, M., Cocks, T. M., & Jenkinson, D. H. (1979) *Nature 282*, 415–417.
Bax, A., & Davis, D. G. (1985) *J. Magn. Reson. 65*, 355–360.
Billeter, M., Braun, W., & Wüthrich, K. (1982) *J. Mol. Biol. 155*, 321–346.
Bodenhausen, G., Kogler, H., & Ernst, R. R. (1984) *J. Magn. Reson. 58*, 370–388.
Bothner-By, A. A., Stephens, R. L., Lee, J.-M., Warren, C. D., & Jeanloz, R. W. (1984) *J. Am. Chem. Soc. 106*, 811–813.
Bundi, A., & Wüthrich, K. (1979) *Biopolymers 18*, 285–279.
Bystrov, V. F., Okhanov, V. V., Miroshnikov, A. I., & Ovchinnikov, Yu. A. (1980) *FEBS Lett. 119*, 113–117.
Chau, M.-H., & Nelson, J. W. (1992) *Biochemistry 31*, 4445–4450.
Chou, P. Y., & Fasman, G. D. (1974) *Biochemistry 13*, 211–222.
Creighton, T. E. (1977) *J. Mol. Biol. 113*, 313–328.
Creighton, T. E. (1978) *Prog. Biophys. Mol. Biol. 33*, 231–297.
Creighton, T. E. (1992) in *Protein Folding: Folding Pathways Determined Using Disulfide Bonds* (Creighton, T. E., Ed.) pp 301–351, W. H. Freeman and Co., New York.
Creighton, T. E., & Goldenberg, D. P. (1984) *J. Mol. Biol. 179*, 497–526.
Davis, D. G., & Bax, A. (1985) *J. Am. Chem. Soc. 107*, 2820–2821.
Dempsey, C. E. (1986) *Biochemistry 25*, 3904–3911.
Dyson, H. J., Rance, M., Houghten, R. A., Lerner, R. A., & Wright, P. E. (1988a) *J. Mol. Biol. 201*, 161–200.
Dyson, H. J., Rance, M., Houghten, R. A., Wright, P. E., & Lerner, R. A. (1988b) *J. Mol. Biol. 201*, 201–217.
Dyson, H. J., & Wright, P. E. (1991) *Annu. Rev. Biophys. Biophys. Chem. 20*, 519–538.
Eigenbrot, C., Randal, M., & Kossiakoff, A. A. (1990) *Protein Eng. 3*, 591–598.
Granier, C., Pedroso Muller, E., & van Rietschoten, J. (1978) *Eur. J. Biochem. 82*, 293–299.
Habermann, E. (1972) *Science 177*, 314–322.
Hore, P. J. (1983) *J. Magn. Reson. 54*, 539–542.
Huyghues-Despointes, B. M., & Nelson, J. W. (1992) *Biochemistry 31*, 1476–1483.
Jeener, J., Meier, B. H., Bachmann, P., & Ernst, R. R. (1979) *J. Chem. Phys. 71*, 4546–4553.
Kemmink, J., van Mierlo, C. P. M., Scheek, R. M., & Creighton, T. E. (1993) *J. Mol. Biol. 230*, 312–322.
Labee-Jullie, C., Granier, C., Albericio, D., Defendini, M.-L., Ceard, B., Rochat, H., & van Rietschoten, J. (1991) *Eur. J. Biochem. 196*, 639–645.
Levitt, M. (1978) *Biochemistry 17*, 4277–4285.

Marion, D., & Wüthrich, K. (1983) *Biochem. Biophys. Res. Commun. 113*, 967–974.
Miroshnikov, A. I., Elyakova, E. G., Kudelin, A. B., & Senyavina, L. B. (1978) *Sov. J. Bioorg. Chem. (Engl. Transl.) 6*, 840–860.
Oas, T. G., & Kim, P. S. (1988) *Nature 336*, 42–48.
O'Neil, K. T., & DeGrado, W. F. (1990) *Science 250*, 646–651.
Osterhout, J. J., Jr., Baldwin, R. L., York, E. J., Stewart, J. M., Dyson, H. J., & Wright, P. E. (1989) *Biochemistry 28*, 7059–7064.
Otting, G., Widmer, H., Wagner, G., & Wüthrich, K. (1986) *J. Magn. Reson. 66*, 187–193.
Pardi, A., Billeter, M., & Wüthrich, K. (1984) *J. Mol. Biol. 180*, 741–751.
Pease, J. H. B., & Wemmer, D. E. (1988) *Biochemistry 27*, 8491–8498.
Rance, M., Sorensen, O. W., Bodenhausen, G., Wagner, G., Ernst, R. R., & Wüthrich, K. (1983) *Biochem. Biophys. Res. Commun. 117*, 479–485.
Shahidi, S., Poronnik, P., Barden, J. A., & Cook, D. I. (1993) *Biochim. Biophy. Acta 1157*, 74–80.
Staley, J. P., & Kim, P. S. (1990) *Nature 344*, 685–688.
States, D. J., Creighton, T. E., Dobson, C. M., & Karplus, M. (1987) *J. Mol. Biol. 195*, 731–739.
van Mierlo, C. P. M., Darby, N. J., Neuhaus, D., & Creighton, T. E. (1991a) *J. Mol. Biol. 222*, 353–371.
van Mierlo, C. P. M., Darby, N. J., Neuhaus, D., & Creighton, T. E. (1991b) *J. Mol. Biol. 222*, 373–390.
van Mierlo, C. P. M., Darby, N. J., & Creighton, T. E. (1992) *Proc. Natl. Acad. Sci. U.S.A. 89*, 6775–6779.
van Mierlo, C. P. M., Darby, N. J., Neuhaus, D., & Creighton, T. E. (1993) *J. Mol. Biol. 229*, 1125–1146.
Vincent, J. P., Schweitz, H., & Lazdunski, M. (1975) *Biochemistry 11*, 2521–2525.
Wagner, G., & Wüthrich, K. (1982) *J. Mol. Biol. 155*, 347–366.
Wemmer, D. E., & Kallenbach, N. R. (1983) *Biochemistry 22*, 1901–1906.
Wishart, D. S., Sykes, B. D., & Richards, F. M. (1991) *J. Mol. Biol. 222*, 311–333.
Wright, P. E., Dyson, H. J., & Lerner, R. A. (1988) *Biochemistry 27*, 7167–7175.
Wüthrich, K. (1986) *NMR of Proteins and Nucleic Acid*, John Wiley & Sons, New York.
Wüthrich, K., Wider, G., Wagner, G., & Braun, W. (1982) *J. Mol. Biol. 155*, 311–319.
Zhong, L., & Johnson, W. C. (1992) *Proc. Natl. Acad. Sci. U.S.A. 89*, 4462–4465.